

Effect of Surface Roughness Height on the Aerodynamics Performance of Axial Compressor Cascade Blades

Assim H. Yousif

Department of Mechanical
Engineering
University of Technology

Jafar M. Hassan

Department of Mechanical
Engineering
University of Technology

*E-mail: Omar_franco64@yahoo.com

Omar A. Khudar*

Ministry of Sciences and
Technology

Abstract

The performance of fluid handling mechanical parts such as compressor blades are usually significantly affected by the surface roughness, because they often operate in condition of peak output that is close to this flow condition. The influence of surface height roughness of compressor blades has been investigated experimentally under the effect of cascade stagger angle. The experimental results done by using the direct measuring technique showed that the aerodynamic coefficients of compressor cascade blades influences by presences of surface roughness and stagger angle. The lift coefficient, pitching moment coefficient and cascade blade efficiency were reduced, while the drag coefficient is increased, with the increase of height roughness. The height of roughness does eliminate the operating condition of the cascade blades, which reduce the value of the stall angle.

Key words: cascade blades, compressor, height roughness, aerodynamic coefficients, stall angle, turbo machine, turbine, wind tunnel.

Introduction

Even in relatively clean environments, a gas turbine may ingest hundreds of pounds of foreign matter each year. Moreover the dusty weather will provide more this amount of particles. These particles of dust are classified into two sizes, particles of size below ($10\mu\text{m}$) which do not cause erosion and particles of size ($20\mu\text{m}$) and above which cause erosion. In general these dusty weathers affect the turbo-engines; therefore the efficiency of these engines will decrease. It means that, the aerodynamic performance is also affected. Dusty weather leads to an extensive roughening of blade surface (reduction in cross sectional area of the compressor blade), so that the compressor performance is usually affected by its surface roughness and eroded parts [1].

The flow past a compressor rough blade has been relatively limited and that very little information about it can be gained by theory alone. Present investigation will be given by a way of information about the effect of surface roughness of compressor performance. The results obtained includes lift coefficient, drag coefficient, pitching moment coefficient and blade efficiency.

Interrelated experimental methods of measurements, such as three electrical weight balance instruments and the static pressure distribution along the blade surface, for both clean and rough surfaces at low, moderate and high stagger angles have been implemented.

(ANSYS Software) is used to simulate the experimental results of the test rig to predict the cascade blade performance in order to achieve the main goals mentioned such us evaluating experimental facilities, instrumentations and measurements techniques used in obtaining the experimental results.

Subsonic wind tunnel

The subsonic wind tunnel used in current experimental program is an open circuit section tunnel with a working cross section of (300 mm x 300 mm) as photographically shown in Figure (1). Wind speeds of (35 m / sec.) are achievable allowing experiments on many aspects of incompressible air flow and subsonic aerodynamics to be performed at satisfactory Reynolds numbers. The tunnel has a smooth contraction fitted with the protective screen. The working section is constructed of clear Perspex with a cross section of (300 mm x 300 mm) and a length of (600 mm). A standard combined Ogival nose pitot-static tube was used to measure reference free stream velocity of the flow in the entrance of the test section. In general the main factors which affect the accuracy of the pitot tube are the turbulence level, velocity gradient, viscosity, misalignment and the vibration on the reading [2].

In the present work, the effect of the viscosity is very small. For the misalignment factor, the errors arise if the pitot head or static head is not accurately aligned with the direction of flow, for small angles the errors are often small. According to National in terms of Physical Laboratory (N.P.L.) standard, the tube is insensitive to quite large angle, for example, at 200 the pressure is only 1% less than at zero angles, the tube is fixed at zero angles, and therefore the error is ignored. The effect of the vibration is avoided by fixing the pitot tube tightly enough and vibration is reduced as much as possible.

Cascade blades

In well designed cascade it is most important to assure that the flow near the central region of the cascade blades (where the flow measurements are made) is approximately two-dimensional. To achieve this, it is preferable to utilize a large number of long blades, but an excessive amount of power would be required to operate the tunnel. With a tunnel of more reasonable size, aerodynamic difficulties become apparent and arise from the tunnel wall boundary layers interacting with the blades [3].

Cascade blades consist of three blades made a circular into arc, Joukowski (25)(0) aerofoil was made from aluminum alloy. The aerofoil span and chord were fixed (290 mm) and (100 mm) respectively and minimum allowable thickness of 1.25 mm. The aerofoil thin thickness is used here to keep the blade thickness acceptable when the sand papers added to both upper and lower blade surfaces (two degree of sand papers of height roughness of 0.192, and 0.317 mm are used).

The leading and trailing edges of the aerofoil are made to form a part of circular that means the entire blade cascade shape is optimized. The blade surface was coated by car varnish in order to make the blade surface as smooth as possible. The cascade model is provided with 15 mm diameter mounting stem and this may be inserted in the bore of the model support and secured by coil tightened with the model clam. Thus the model support may be adjusted at the desired stagger angle. In the present investigation, the percentage cascade frontal area to the test cross-sectional area is 2%. According to [4], this means that the blocking errors are relatively small and may be negligible.

The geometric parameters of the cascade are listed in table (1). The cascade nomenclature is illustrated in Figure (2).

Table (1): Cascade Geometry

Blade Chord (c)	Aspect Ratio	Solidity (a = s/ c)	Blade Number	Camber Angle	Pitch Spacing(s)			
100 mm	2.95	0.75	3	24°	73.5 mm			
Stagger Angle (y) Variety								
0°	3°	6°	9°	12°	15°	18°	21°	24

Pressure distribution measurements

The lift and drag coefficients can be measured for isolated blade (mid blade of the cascade), by measuring the pressure distribution on the blade surfaces of the cascade. For this purpose, the blade is provided with ten orifices (static holes tapping), have (0.75mm) a diameter, care being taken to make the static holes flush to surface and to insure that holes are with right angles to surface to minimize the reading errors [5]. Each is individually

connected to a tube of a multi-tube manometer. Therefore the mid blade is connected to ten pressure tapping by means of which the pressure distribution around the blade at any stagger angle may be measured. Pollard, [6] shows that the performance of compressor cascade blades varies little between Reynolds number based upon the blade chord of 1.1×10^5 and 2.6×10^5 . At this stage it is convenient to run the tunnel at maximum speed (35 m/sec) to give Reynolds number of order (2.6×10^5) .

Numerical investigation

At the present investigation ANSYS is used to solve the flow governing equations. The governing equations are the continuity, momentum and energy equation for steady, incompressible, two-dimensional viscous flow.

The computational solution using ANSYS flotrán has been applied using the following steps [7]:

- 1- Determining the problem domain.
- 2- Determining the flow regime which concerns flow characteristics.
- 3- The boundary conditions, which concerns in the velocity of blades and the wall of wind tunnel.
- 4- Physical considerations.
- 5- Reductions of the problem to a set of linear algebraic equations.

Aerodynamic coefficients calculations

The aerodynamic coefficients can be calculated according to [8] from predicted or measured blade pressure distribution. Total force (z) exerted on the isolated blade can be obtained by using the following relations:

$$z = \int_0^c -(P - P_o) dx + \int_0^c (P - P_o) dx \quad \dots(1)$$

Using subscripts (u) and (L) for the upper and lower surface respectively, this becomes

$$z = -\int_0^c [(P - P_o)_u - (P - P_o)_L] dx \quad \dots(2)$$

Equation (2) is easily put into coefficient form as follows as given in [8].

$$C_z = \frac{z}{\frac{1}{2} \rho v^2 s} \quad \dots(3)$$

Considering unit span, the area (s) is equal to the chord (c), therefore the total pitching moment due to (z) is

$$C_{Mz} = +\int_0^c (C_{Pu} - C_{Pl}) \left(\frac{x}{c}\right) d\left(\frac{x}{c}\right) = -\int_0^c \Delta C_P \left(\frac{x}{c}\right) d\left(\frac{x}{c}\right) \quad \dots(4)$$

$$C_M = \frac{M}{\frac{1}{2} \rho v^2 s c} = \frac{M}{\frac{1}{2} \rho v^2 c^2} \quad \dots(5)$$

The contribution to CM due to x-force may be obtained as

$$C_{Mz} = \int_{z_1/c}^{z_2/c} \Delta C_P \left(\frac{z}{c}\right) d\left(\frac{z}{c}\right) \quad \dots(6)$$

The force coefficient (Cx) and (Cz) are parallel and perpendicular to the chord line, whereas the more suitable coefficients CL and CD are referred to the air direction. The conversion from one pair to the other may be performed by reference to Fig. (3), in which CR is the coefficient of resultant aerodynamic force, acts at an angle (γ) to (Cz). CR is the resultant of both (Cx) and (Cz), and of (CL) and (CD), and therefore, from the Figure (3).

$$C_L = C_R \cos(\gamma + \alpha) = C_R \cos \gamma \cos \alpha - C_R \sin \alpha \sin \gamma \quad \dots(7)$$

and

$$C_R \cos \gamma = C_z \quad \text{and} \quad C_R \sin \gamma = C_x \quad \dots(8)$$

Where

$$C_L = C_z \cos \alpha - C_x \sin \alpha \quad \dots(9)$$

Similarly

$$C_D = C_R \sin(\alpha + \gamma) \text{ or } C_D = C_z \sin \alpha + C_x \cos \alpha \quad \dots(10)$$

Efficiency of compressor cascade

The efficiency (η) of the cascade blades can be defined in the same way as that of diffuser efficiency; which is the ratio of the actual static pressure a cross the cascade to the maximum possible theoretical pressure rise (i.e. with zero lift drag (Dp0=0) as given in [9], Therefore:

$$\eta_D = 1 - \frac{2C_D}{C_L \sin 2\alpha_m} \quad \dots(11)$$

Where (αm) is the mean flow angle and the optimum mean flow angle for maximum efficiency is (αm)=45, thus equation (12) can be written as: (12)

Direct measurements of aerodynamic coefficients

An electric three component weight balance was used to measure lift, drag forces of the cascade blade and pitching moment directly, it was designed and manufactures to suit the present investigation.

Figure (4) shows photographically the electrical three Component Weight devices. The instrument is designed for flow flows from right to left when it is viewed from the front. The balance is constructed mainly from aluminum alloy and its main

framework comprises a base plate which is secured to the wind tunnel working section three studs and with carries a triangular force plate. The force plate and base plate are connected with three supporting legs, disposed at the corners of the force plate, the effect of this, is to constrain the force plate to move in plane parallel to the base plate. Each leg is attached to the force plate and base plate by spherical universal points. The effect of this is to constrain the force plate to move in plane parallel to base plates. While leaving it to rotate about a horizontal axis; the necessary three degrees of freedom are thus provided. The instrument is provided with (15 mm) diameter mounting bore to support the model and the model is secured by coiled tightened by the model clam. The model support is graduated on the peripheries and is free to rotate in the force plate for adjustment at the angle of incidence of the model, while its position may be located by means of an incidence clamp.

The force plate may be locked in position by two centring clamps, and these should always be tightened when the balance is not in use or when changing models. It is provided with a spirit level for initial setting up of the balance, and for adjustment being made. The force acting on the force plate is balanced by electrical load cell type LPX 250, nominal output at capacity 2 mv/v, recommended excitation 5v~20v AC /DC of cantilever from the drag load cell, the lift force load cell and the aft lift load cell. The variation in atmospheric temperature, pressure, humidity, and vibration does not affect the output signal of the load cell [10]. Forces are transmitted from the plates to the load cell by way of thin beryllium copper taps and knife edges the drag tapes which lie horizontally. Action line through the centre of the model support, while the two lift taps act vertically through points disposed equidistantly from the centre of the model support and the same horizontal plane as the support.

The distance between the right and aft lift tapes of the device is (15 cm), and the sum of the forces in these tapes thus gives the lift on the model, while the difference, when multiplied by distance gives the pitch moment (Nm). The weight balance has been designed to measure maximum lift of 2KN at wind speed of 100 m/sec.

Results and discussion

Figures (5, 6 and 7) represent the variation of lift coefficients with the change of stagger angle (γ), while Figures (8, 9 and 10) represent the variation of drag coefficients with (γ), both for clean and rough surfaces. These figures indicated that the lift and the drag coefficients from direct measurement (three weight balances), from measuring the

pressure distribution on the blade surfaces and numerically using CFD code. Figures (5 and 8) show that the lift and drag coefficients variations with (γ) gave as expected common behavior of such variation for clean blade. The measured and calculated (C_L) values were seems to be in reasonable agreement. Figures (6, 7, 9 and 10) show that the direct measured technique of (C_D and C_L) are higher LCLC than the other results for all rough surfaces to be investigated especially the calculated values from measured pressure distributions. These differences are due to that the (C_D) values calculated from pressure distributions do not include the induced drag; they only took into account zero lift drag. Also these differences may be due to the effect of fixing sand papers on the blade surfaces, in which they used to simulate the surface roughness on the reading of the static pressure. The static pressure measurements using static tapping are very sensitive to the surface roughness and flashiness of the holes with the blade skin. This sensitivity is due to the generation of vortex in the turbulent boundary layer (inner region) close to the surface [11]. The main conclusion raised from the former results is that the direct measured values of lift and drag coefficients were gave the best measured coefficients close to the real values and gave a smooth and gradual variations of drag for all cases with (γ). Also Figures (5, 6 and 7) showed that stall stagger angle for each surface being steadied (clean and rough surfaces) are the same for three weight balance, pressure distribution and ANSYS results. DC

Figure (11) shows the variation of measured lift coefficient using direct technique with (γ) for clean and rough surfaces. In all cases been examined the lift coefficient increase gradually till a stall values of (γ). This Figure shows that the lift coefficients are reduced with the presence of surface roughness, this reduction increases with increase of high roughness. Rough surfaces also affect the flow so that the action will progress and augments, therefore boundary layer separation and stall move upstream and give pressure loss greater than the clean surfaces. The height of roughness does eliminate the operating condition of the cascade blades, which reduce the value of the stall angle and this reduction increase with the increase of height roughness. Stall stagger angles are (220, 160 and 120) for clean and rough surfaces.

Figure (12) shows that the variations of drag coefficient with (γ) for clean and rough surfaces. This Figure shows a slight effect of existing of surface roughness on the drag coefficient variation. The variation of height roughness shows a very slight influence on drag coefficient variation.

Figures (13) represent the variation in pitching moment coefficient with (γ). The pitching moment coefficient increases with increase (γ). The results show a reduction in the pitching moment coefficient with the presence of the surface roughness. This reduction increases with increase of height roughness. At the critical (γ) angles (γ_c) values jumps suddenly to relatively higher values and this may be due to the early occurrence of the flow separation at the blade suction side at high (γ). MC

Figure (14) shows the variation in cascade blade efficiency with (γ). The cascade blade efficiency decreases with increasing (γ) values. Surface roughness will affect the skin friction drag and this leads to increase the wall shear stress, which causes increase in the pressure loss coefficient and drag force. The presence of surface roughness shows a reduction in the cascade efficiency, therefore this indicates that the efficiency is inversely proportional to (γ), and to degree of roughness.

The present investigation of the cascade performance characteristics for rough cascade blades showed a reduction in the lift coefficient and blade efficiency as compared with those of clean cascade blades. The drag coefficient is increased as the height roughness is increased. These results are agree well with result obtained by [12], with more confidence output data, since the present direct measuring technique is recent and most sophisticated technique used in such measurement.

Conclusion remarks

It has been observed that there is a reduction in lift coefficient pitching moment coefficient, and efficiency, while the drag coefficient is increased with the increase of the surface height roughness. The height of roughness does eliminate the operating condition of the cascade blades, which reduce the value of the stall angle and this reduction increase with the increase of height roughness.

At critical stagger angles near the stall angle, the pitching moment coefficient will jump suddenly to relatively higher values due to the advance of flow separation at high stagger angles

Nomenclature

C	chord	m
CD	Drag Coefficient	-
CL	Lift Coefficient	-
CM	Pitching moment coefficient	-
CR	Resulting of aerodynamic forces	N
Cx	Force coefficient parallel to chord line	-
Cz	Force coefficient perpendicular to chord line	-

Po	Upstream static pressure	N/m ²
s	Pitching spacing	m
S	Area	m ²
U	Velocity component at x-direction	m/ sec
V	Velocity component at y-direction	m/ sec
Z	Total force	N
α_1, α_2	Inlet and outlet flow angles	deg.
β_1, β_2	Inlet and outlet blades angles	deg.
Γ	Stagger angle	deg.
P	Density	kg/m ³
σ	Solidity	-
η	Efficiency of cascade blades	-

References

- 1-Loud R. L. and Staterpryce, A. A. Gas Turbine Inlet Air Treatment, Gas Turbine Power Plant System, GE Company, 1991.
- 2- Hawthorne, R. W., Aerodynamic of Turbine and Compressors, Oxford University Press, London, 1969.
- 3- Dixon, S. L., Fluid Mechanics, Thermodynamics of Turbo Machinery, Program Press, fifth Edition, 2003.
- 4- Maskel, C. E., "A Theory of Blockage Effects of Buff Bodies and Stalled Wings in A Closed Wind Tunnel, ARCR & M 3400, 1965.
- 5- Owen, ZE. and Paukhurst, R. C., Measurement of Air Flow, 5th edition, London, 1970.
- 6- Pollard, Some Experiments at Low Speed on Compressor Cascade, ASME Journal of engineering for power, July 1967, PP.427-436.
- 7- ANSYS Theory Reference, 000855, Eight Edition, SAS I.P., Inc. 2003
- 8- Houghton, E. L. and Carpenter, P. W. Aerodynamics for engineering students, Fifth edition, the University of Warwick, Butterworht-Heinemann, an imprint of Elsevier science, 2003.
- 9- Bo Song, Experimental and Numerical Investigations of Optimized High-Turning Supercritical Compressor Blades, Blacksburg, Virginia, November, 2003.
- 10- Yousif, A. H., An Analytical Approach in Turbulent Analysis at Separation for Bubble Tripping, Eng. Technology Suppl. No.3, Vol.20, 2001.
- 11- Yousif A. H., The Separation of Flow Tripped, 2-D Turbulent Boundary Layer ,Journal of Baghdad University, volume 6, No.1, 2000.
- 12- Yousif, A. H., Al-Fatth, I. A. and Abid, A. B., Effect of Roughness on the Performance of Axial Compressor Cascade, MTC Journal .No.4, 1989.

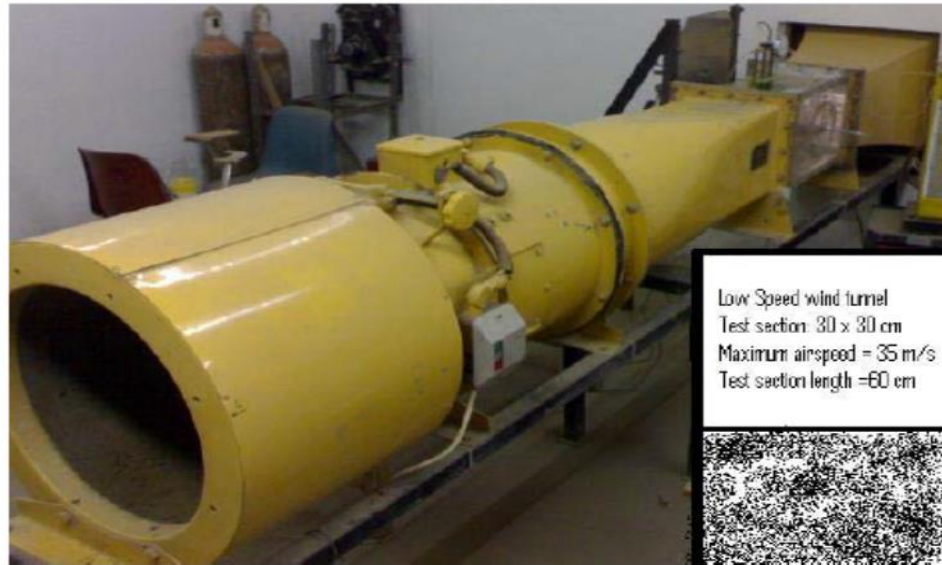


Figure (1):Low speed wind tunnel

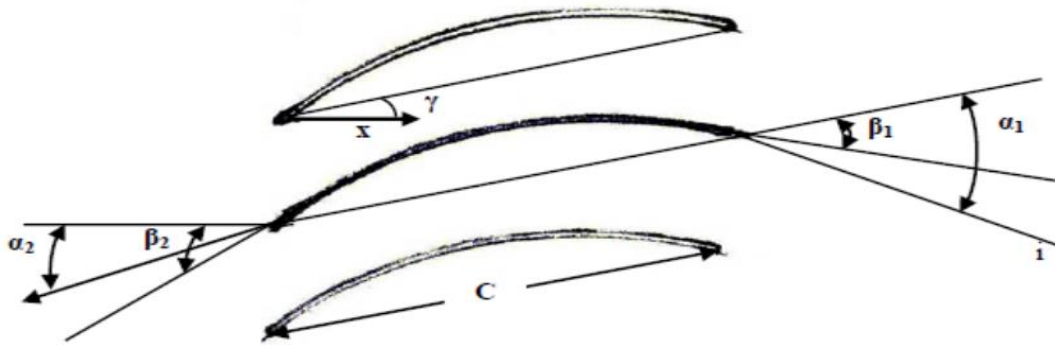


Figure (2): Cascade nomenclature

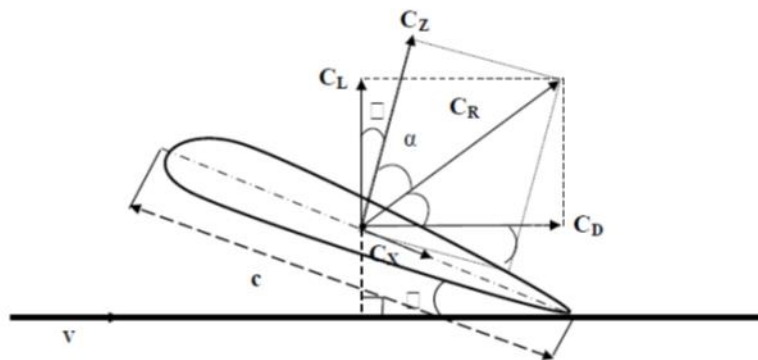


Figure (3): Aerodynamic bluff body with Aerodynamic Coefficients



Figure (4): Electrical three weight balance

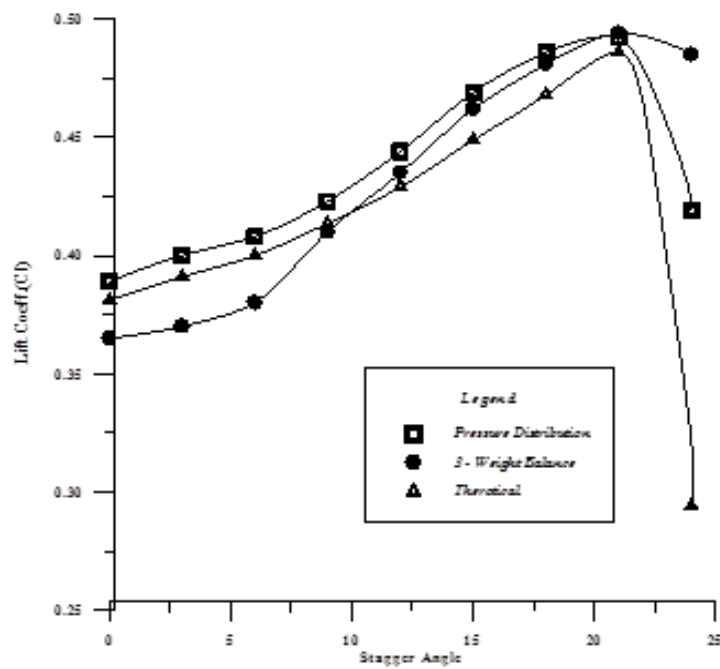


Figure (5): Lift coefficient versus cascade stagger angle, clean blades surfaces ($v=35\text{m/sec}$ and $Re=2.6 \times 10^5$)

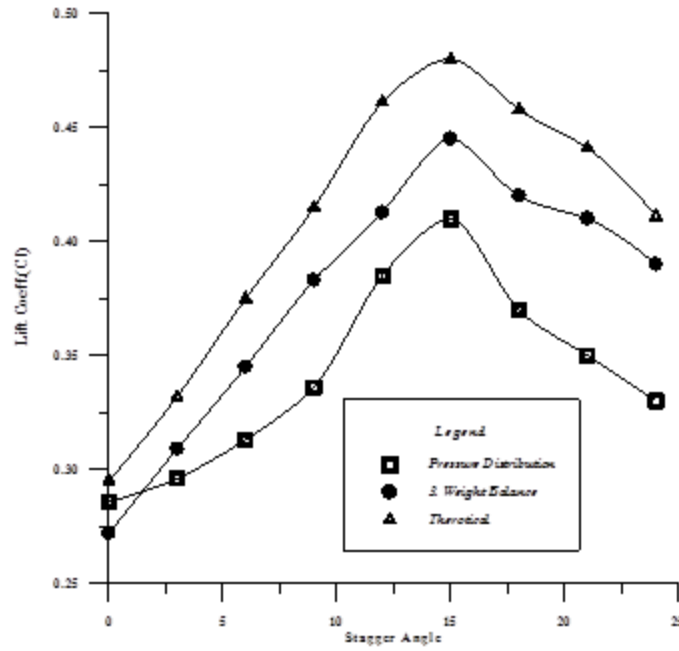


Figure (6): Lift coefficient versus cascade stagger angle, blades surfaces height roughness=0.192mm (v=35m/sec and Re=2.6 x10⁵)

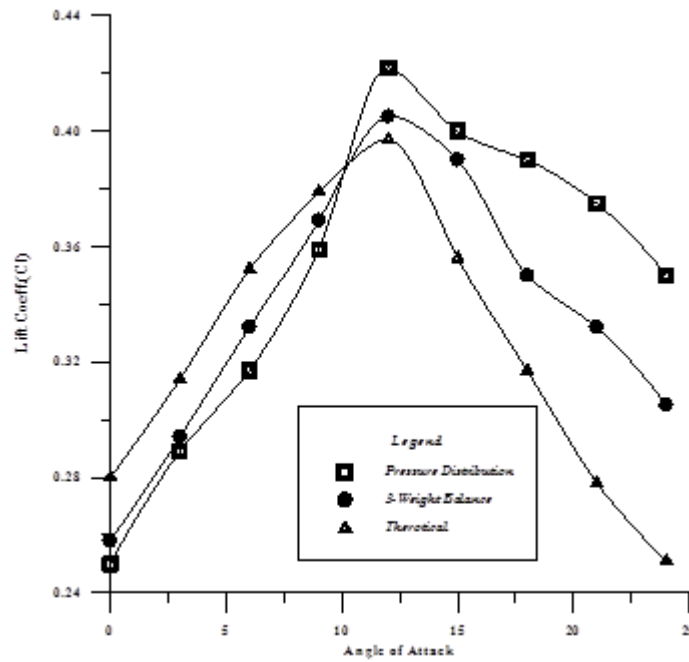


Figure (7): Lift coefficient versus cascade stagger angle, blades surfaces height roughness=0.317mm (v=35m/sec Re=2.6 x10⁵)

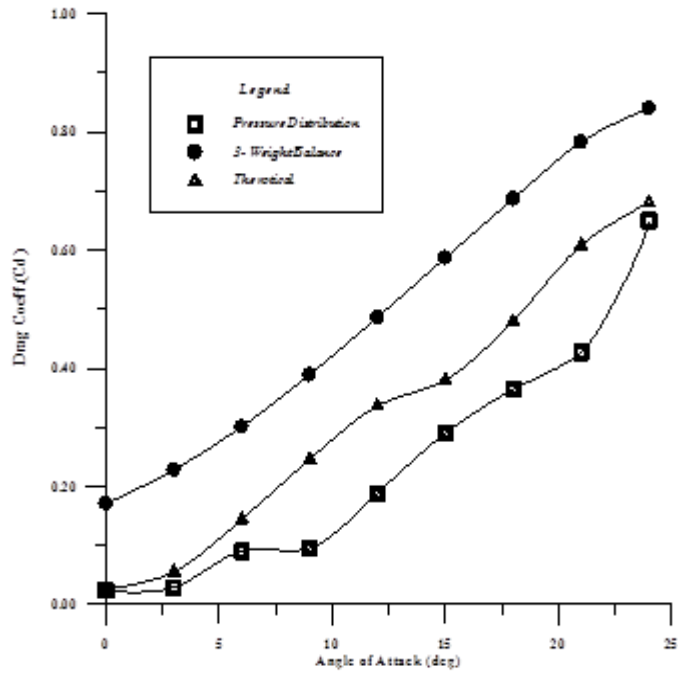


Figure (8): Drag coefficient versus cascade stagger angle, clean blades surfaces ($v=35\text{m/sec}$ and $Re=2.6 \times 10^5$)

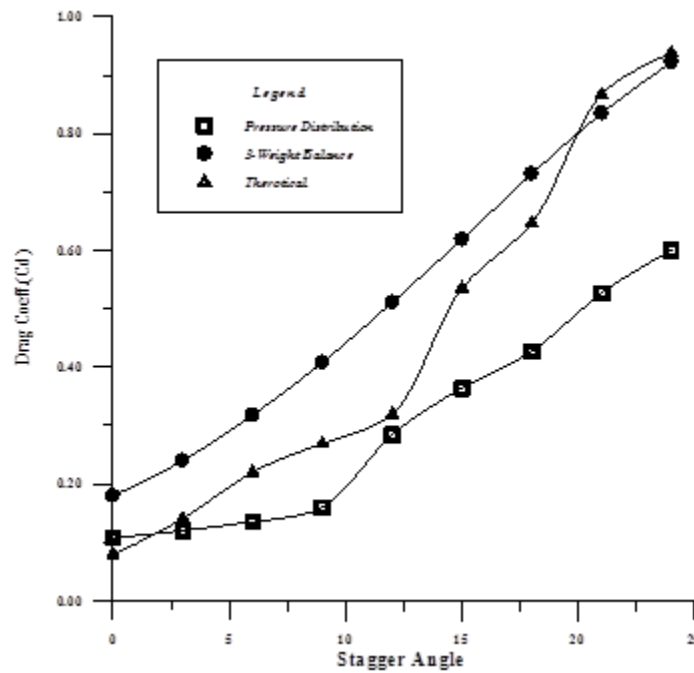


Figure (9): Drag coefficient versus cascade stagger angle, blades surfaces height roughness=0.192mm ($v=35\text{m/sec}$ and $Re=2.6 \times 10^5$)

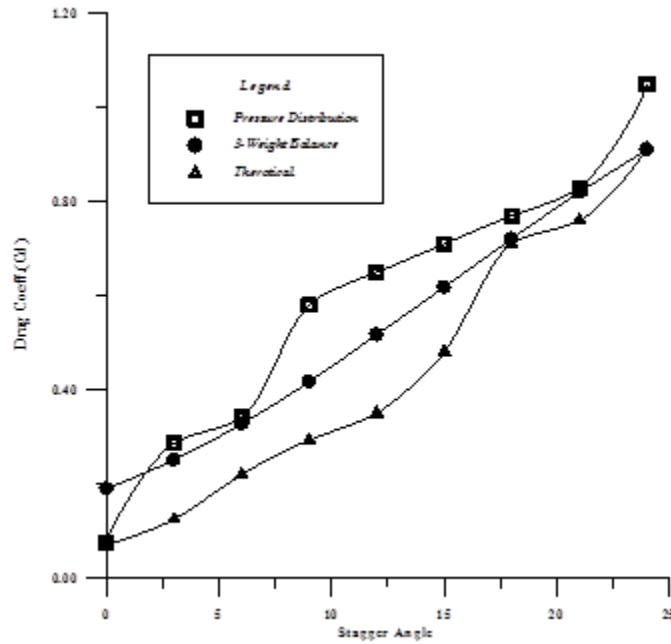


Figure (10): Drag coefficient versus cascade stagger angle, blades surfaces height roughness=0.317mm ($v=35\text{m/sec}$ and $Re=2.6 \times 10^5$)

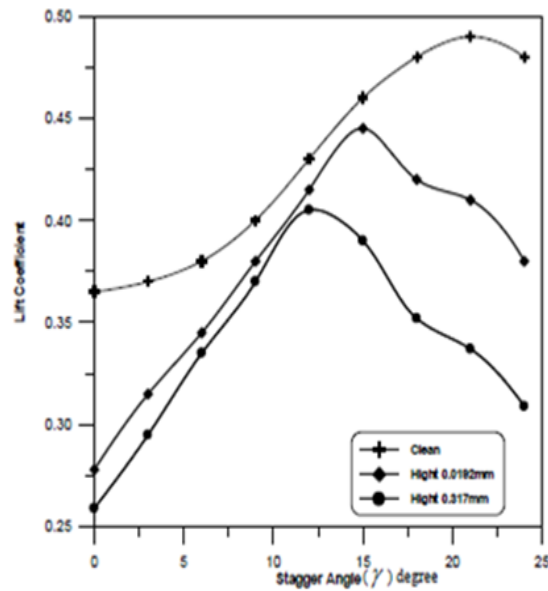


Figure (11): Lift coefficient versus stagger Angle. Three weight balance three weight balance technique ($v=35\text{m/sec}$ and $Re=2.6 \times 10^5$)

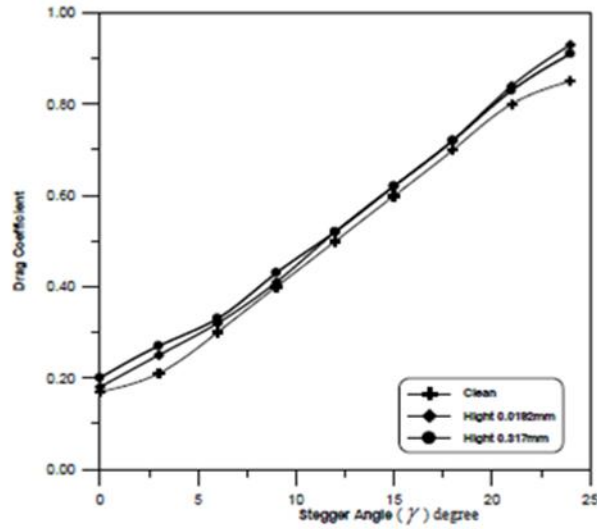


Figure (12) Drag Coefficient versus Stagger Angle ($v=35\text{m/sec}$ and $Re=2.6 \times 10^5$)

Figure (12): Drag coefficient versus stagger Angle ($v=35\text{m/sec}$ and $Re=2.6 \times 10^5$)

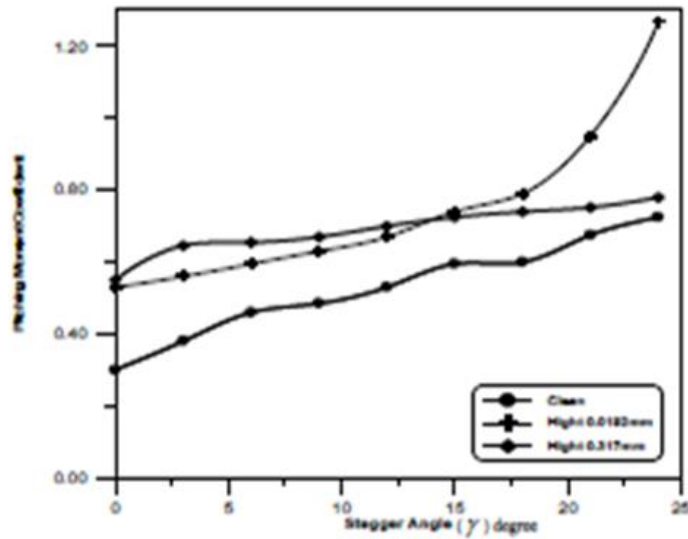


Figure (13): Pitching Moment coefficient versus stagger Angle ($v=35\text{m/sec}$ and $Re= 2.6 \times 10^5$)

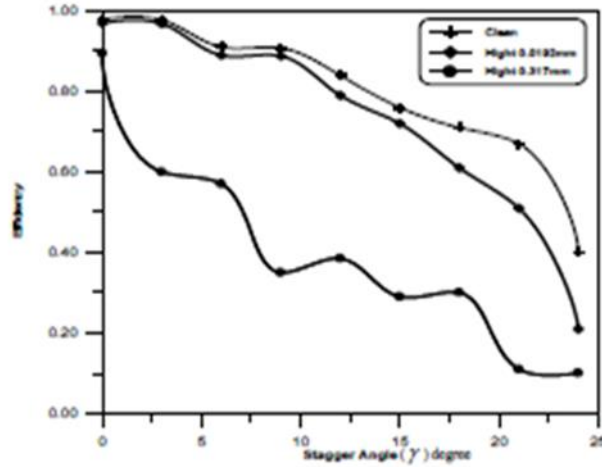


Figure (14): Efficiency Stagger Angle ($v=35\text{m/sec}$ and $Re= 2.6 \times 10^5$)

تأثير ارتفاع الخشونة السطحية على الاداء الايروديناميكي لصف من الزعانف لضغط

محوري

عمر عبد الرزاق
وزارة العلم والتكنولوجيا

جعفر مهدي حسن
قسم الهندسة الميكانيكية/ الجامعة التكنولوجية

عاصم حميد يوسف
قسم الهندسة الميكانيكية/ الجامعة
التكنولوجية

الخلاصة:

ان اداء الاجزاء المتحركة كزعانف الضاغط تتأثر بالخشونة السطحية وان ارتفاع الخشونة السطحية لأسطح زعانف الضاغط يظهر جليا و واضحا في صف من الزعانف موضوعة تحت تأثير نفق هوائي. وقد بينت النتائج العملية التي تم قياسها مباشرة بطرق تقنية ان المعاملات الايروديناميكية للزعانف مثل (معامل الرفع، معامل عزم التعرج، كفاءة الزعانف) تتغير مع زيادة الخشونة السطحية كما ان معامل الكبح نحو الإعاقة يزداد مع زيادة الخشونة. لذلك فإن زيادة الخشونة السطحية تعمل على نقصان زاوية الانهيار مما يؤدي بالنتيجة الى إضعاف أو القضاء على ظروف عمل الزعانف.